June 23, 2011

Comparison of Azimuthally Varying with Constant Gradient Magnetic Fields with the Rutgers 12-Inch Cyclotron

Timothy W. Koeth, George A. Hine, Daniel E. Hoffman, James E. Krutzler, Timothy S. Ponter, Aaron J. Rosenberg, Kiersten J. Ruisard, William S. Schneider,
Rutgers University, Piscataway, NJ, 08854

ABSTRACT The Rutgers 12-Inch Cyclotron is a 1.2 MeV particle accelerator dedicated to beam physics instruction as well as accelerator component research and development.[1] The cyclotron is uniquely suited to study the beam dynamics under different pole tip configurations. The 12-inch magnet was initially fitted with parallel magnetic pole tips creating uniform vertical magnetic field in the useable region of ion acceleration, however the resulting field lacked focusing properties. The next set of pole tips studied has a constant radial decrease of the vertical field.[2] The focusing technique known as weak focusing brought the accelerator beam to the periphery.[3] A final set of pole tips were constructed that cause the vertical magnetic field to vary with azimuth at given radius. Such tips provide axial focusing which can significantly exceed the weak focusing field. In this paper we will cover simulations and measurements of the magnetic fields for the existing 'weak focusing,' trial Azimuthally Varying Field (AVF) pole tips, and an optimized set of AVF pole tips expected to bring a proton beam to the periphery.

INTRODUCTION The cyclotron's magnetic field bends the accelerated ion beam in a circular orbit, iteratively returning the ions to the accelerating gap. Neglecting relativistic mass increase, the cyclotron equation,

$$f_{cyc} = \frac{qB}{2\pi m},$$

indicates that the revolution frequency of an ion is independent of the radius. Although it would appear desirable to have a uniform vertical magnetic field over the entire region ion acceleration in order to keep the revolution frequency in step with the frequency of the applied oscillating high voltage, this is not practical in operation; any ion that begins with the slightest angle of inclination (or declination) with respect to the accelerating plane in such a field will spiral up (or down) and terminate on the chamber lids before reaching the target. A restoring force is needed to return wandering ions to the accelerating plane.

The first method to provide such a restoring force was found by slightly reducing the vertical magnetic field as the pole tip radius increased. This is accomplished by a machining the pole tips with a slight conical taper. Envisioning the field lines in the magnet gap, as viewed from the side view, the reader sees them slightly bulging outwards from the center, as depicted in Figure 1. By, $\vec{\nabla} \times \vec{B} = 0$, the bulging causes a radial *B*-field component that grows in strength with offset height above and below the accelerating plane. Because the accelerating plane is now symmetrically seated between the upper and lower volumes of magnetic field which contain a radial component, it is referred to as the median plane. The B-field is strictly vertical in the median plane.

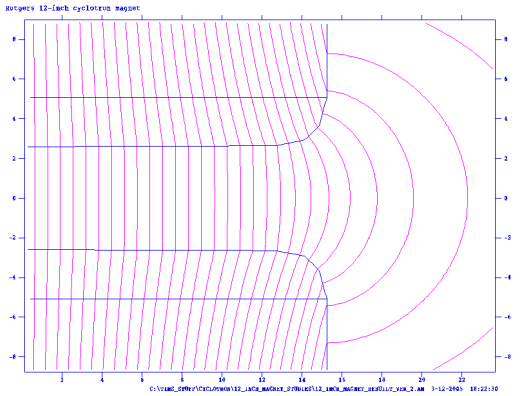

Figure 1. Field lines of weak focusing poles viewed from the side.

With this construction, the vertical field has a dependence on radius, $B_z(r)$, and so too does the cyclotron frequency, $f_{cyc}(r)$. Since the RF system typically operates at one frequency, there will be a mismatch between f_{cyc} and f_{RF} for most r. This mismatch is further exacerbated when relativistic mass increase is considered.

The focusing force generated by the sloping poles is known as 'weak focusing,' one might then anticipate there being a stronger focusing mechanism. However Thomas proposed a magnetic field configuration, which not only

would provide comparable focusing, but it would also accommodate relativistic effects.[4] In the Thomas field, focusing is accomplished by an azimuthally varying field (AVF) where the average vertical magnetic field is permitted to grow with radius so as to keep the relativistic mass increase in step with the fixed frequency of the RF system.

The distinction between focusing strengths is defined by the number of transverse oscillations a particle will make per revolution in the accelerator; a value also referred to as the *tune*, ν_z, ν_r. Any accelerator in which the orbiting particle executes less than one transverse oscillation per revolution is considered 'weak' focusing and any machine where the number of transverse oscillations is greater than one per revolution is in the 'strong' focusing regime. Our exploration with AVF poletips will be in intermediate regime where the axial focusing can be stronger than the weak focusing pole tips. Such poletips will have vz <1 and vr~1; the radial tune may exceed unity under certain circumstances.

To gain a deeper illumination on the focusing properties of azimuthally varying fields, the Rutgers 12-Inch cyclotron has constructed two sets of AVF poletips for experimentation.

The first set was a simple, pure-radial sector design of periodicity four. Their geometry was the least expensive to machine and provided the maximum field variation achievable within practical constraints. Not expected to host beam, their purpose was to benchmark simulations, measurement techniques, and test analysis code.

The second set of AVF poletips are the product of an ambitious design program assigned to the Spring 2011 *Cyclotron Students*. Using the design tools developed with the pure radial sector poles, the second set, employing an Archimedes spiral, is expected to successfully transport beam from the ion source to the periphery.

As a consequence, this paper treats the two AVF pole tips as separate experiences. First, the radial sector investigation was a didactic program to develop the necessary tools for the second set of poletips – an earnest design program with the goal of accelerating beam. Second, the AVF poletips

AVF FOCUSING The axial restoring force in the constant gradient 'weak' focusing poles results from the interaction of the ions' angular velocity component with the radial magnetic field component above and below the median plane; mathematically stated as $F_z=qv_\theta B_r$. The angular velocity, v_θ, is proportional to the particles' kinetic energy and, as noted earlier, B_r is proportional to the magnetic field gradient, on which stability requirement places limits.[2]

In the radial sector AVF, the vertical restoring force arises from the ion's radial velocity interacting with the magnetic field's azimuthal component, $F_z = qv_rB_\theta$. [5] There are then two parameters contributing to the AVF axial restoring force: v_r and B_θ. First, the ion's radial velocity component, v_r, is generated by the change in vertical field strength between hill and valley regions – this will be seen as scalloping of circular orbits. The *rms* variation of the vertical field is called flutter and is denoted as *F*. The azimuthal magnetic field component, B_θ, is also proportional to the flutter.

The axial focusing can be further enhanced by instantaneously tilting the sector edge. Continuously applying an edge angle will result in a spiral sector edge from the center to the periphery. The instantaneous angle that the sector edge makes with the orbit is ξ. The tilting of the sector edge, projects a portion of the radial sector's B_θ component into the radial direction:

$$B_r = -B_\theta \tan(\xi),$$

invoking another $qv_\theta B_r$ force. Note that this B_r is separate from the weak focusing B_r.

AVF focusing can be used to supplement weak focusing. In this context, the weak focusing comes from the average radial gradient's field index, denoted as *k*, where:

$$k = \frac{d \ln \langle B \rangle}{d \ln R}.$$

The tune is proportional to the relative focusing strength. Following the treatment of J.J. Livingood,[6] one can write the axial tune in terms of the average field index, flutter, and the instantaneous edge angle:

$$\nu_z^2 = -k + F(1+\tan^2\xi)$$

The radial tune is written as

$$\nu_r^2 = 1+k$$

A balance is sought in the design of AVF pole to maximize v_z for the entire duration of the ions path, while avoiding destructive resonances associated with integer and rational fractional values of both v_z, and v_r.

FIELD MEASUREMENTS To validate the magnet simulations, measurements of the vertical B-field component were performed for several pole tips. Previously, 2D Possoin-Superfish models were created of the weak focusing pole tips, and a corresponding 2D B_z-field scan was performed. We revisit the old measured data with our new analysis tools before we turn our attention toward the measurement of AVF Bz-fields.

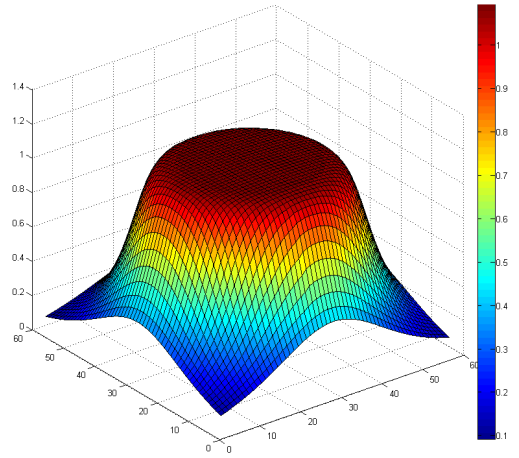

Figure 2. Old B_z measurement data of a 2-D scan of the weak focusing pole tips plotted with new analysis code.

Weak focusing The weak focusing pole tips have already been studied [2], however we returned to the measurements with the MatLab code prepared to analyze the AVF field measurements. We were then able to test the MatLab Code for the pending AVF analysis.

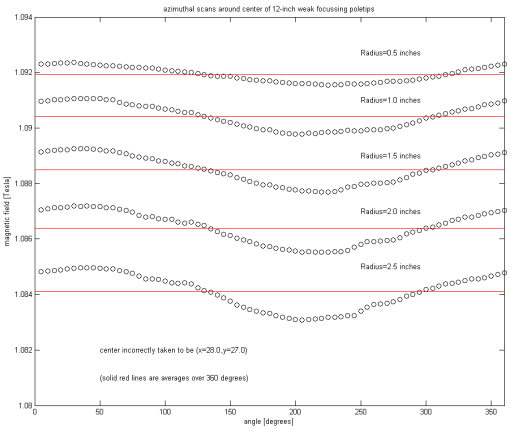

Figure 3. Plotting B_z as a function of azimuth at several radii – the circles are the data points, the red lines are the average B_z values.

Poor beam intensity motivated our search for an undesired azimuthal variation of periodicity two, which resulted in the 2-D B_z-field measurements of the weak focusing field shown in Figure 2. Since no detectable azimuthal variation was found, our quest to improve the beam intensity led us in other directions, including the ion source. [7]

The newly written MatLab analysis code plots B_z about a circle of any requested radius in 5° increments – the center of the circle is intuitively chosen. Although the data lies on a rectangular grid, a MatLab provided 2-D linear interpolation routine was used to determine the field at any requested location. Plotting B_z as a function of angle for several radii reveals a sinusoidal variation, as shown in Figure 3. It is evident that the magnetic center is within the bounding circle, but not concentric with it. The averaged B_z of each measurement circle is also plotted in Figure 3 as a red line.

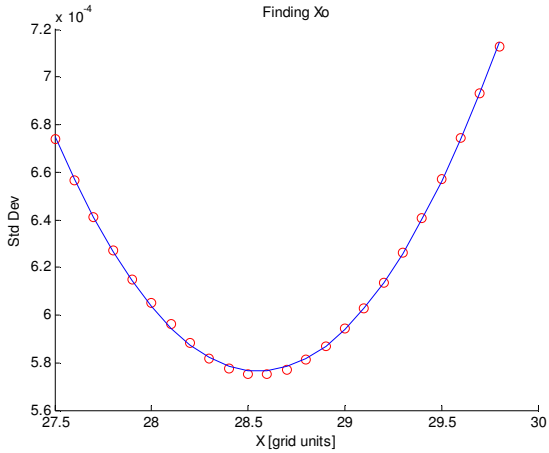

Figure 4. The magnetic center was found by finding the minimum standard deviation of the Bz-field values for different analysis circle's center X-, and Y-positions.

In the weak focusing case, the magnet center was determined by sweeping the center of the circle first in the *x* and then the *y* directions. The standard deviation of the values about the measurement circle was calculated and stored. After a sweep in *x* or *y* that included the magnet center, the data was fit to a parabola, from which the minimum standard deviation, *i.e.* the center locations, could be inferred as seen is Figure 4.

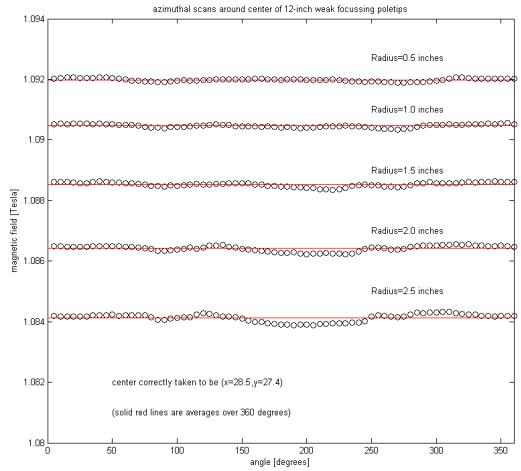

Figure 5. Plotting B_z as a function of azimuth at several radii after finding magnetic center.

Once the centers were evaluated, the analysis code was updated. The centering routines were independently performed for each chosen radius

– i.e. evaluation circle. The azimuthal analysis was then repeated, and the results are shown in Figure 5. Clearly each measurement point lies much closer to the average than was depicted in Figure 3. Comparison of the centers determined from the fit, show that the field is axisymmetric to 4 parts in 10,000.

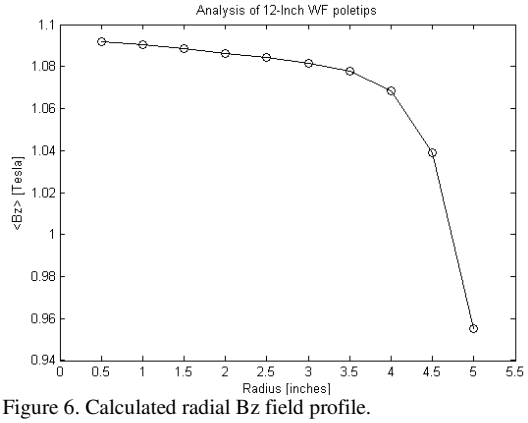

Figure 6. Calculated radial Bz field profile.

The average radial field profile, plotted in figure 6, is generated from the assembled average fields along the radius – this is needed to calculate the average field index, *k*. In the case of the axisymmetric weak focusing field, the average field index is the same as the instantaneous field index, *n*.

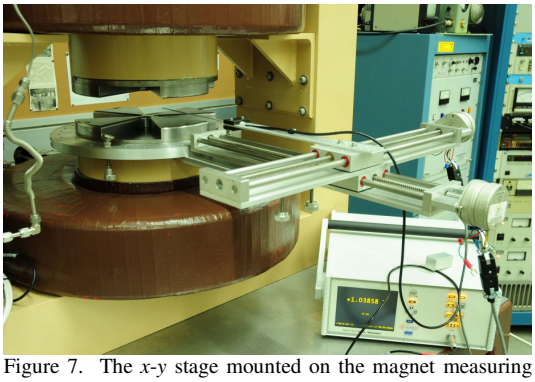

Figure 7. The *x*-*y* stage mounted on the magnet measuring the radial sector AVF poles.

Radial AVF Measurements. It was important to systematically measure and reproduce the vertical B-field component at median plane for the AVF studies. Our group custom designed and built a computer-controlled stepper-motor driven X-Y stage which utilized zero-backlash acme threads to sweep a magnetic field probe through the median plane. An F. W. Bell 7010 hall probe based gauss meter was used for the AVF measurements; the gauss meter was outfitted with an RS232 data port. The computer program which controlled the X-Y stepper motors also recorded the gauss meter data, fully automating the measurement process. An overall view of the measurement apparatus is shown in Figure 7. A Programmable Logic Controller (PLC) based machine-protection system was implemented to allow safe, un-attended operation of the 12-Inch magnet. In the event of high-temperature condition or a coil cooling-water flow loss for more than 10 seconds, the PLC will slowly ramp the magnet down and latch it off, requiring an operator to reset. The PLC safety system was necessary as the scans could take in excess of 24 hours: a standard measurement grid of 129 x 129 points equals 16,641 measurement points, each measurement required ~ 5 seconds totaling an excess of 23 hours scan time.

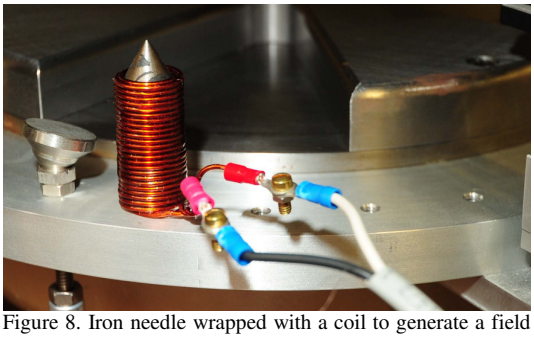

Figure 8. Iron needle wrapped with a coil to generate a field bump for position calibration.

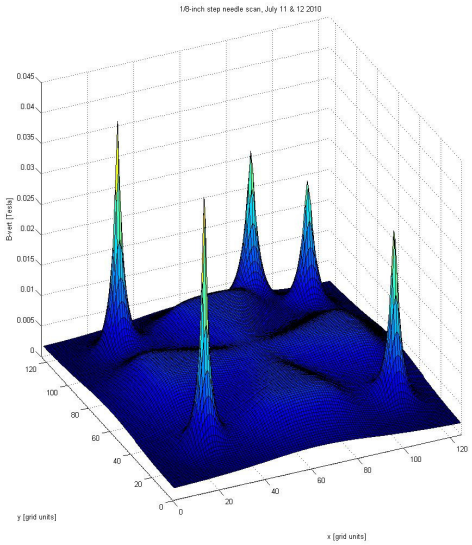

Figure 9. Data from field bump scan – note residual magnetization in the 12-Inch AVF poles.

To calibrate the hall probe's position against the magnet's mechanical center, magnetized iron needles were precisely placed around the pole tip to create field bumps, one such needle is displayed in Figure 8. The field-bump calibration was performed with the 12-Inch magnet de-energized. A full 2-D scan was completed; peaks found by fitting to the measured field bump were

taken to be the center location of the needles and calibrated to the X-Y stage position.

A result of a of field-bump calibration scan is shown in Figure 9, it also reveals the residual magnetization of the 12-Inch magnet. Four needles were needed to scale both dimensions; the fifth needle was used to break the symmetry, removing orientation ambiguities.

The variation of the peak amplitudes indicate the probe was traveling in a plane slightly tilted with respect to the median plane. However, this effect seems to be insignificant in the measurement of actual AVF field. A vertical sensitivity study will be done.

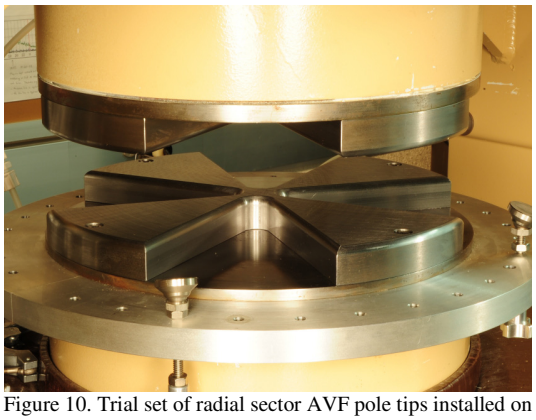

Figure 10. Trial set of radial sector AVF pole tips installed on the 12-inch magnet.

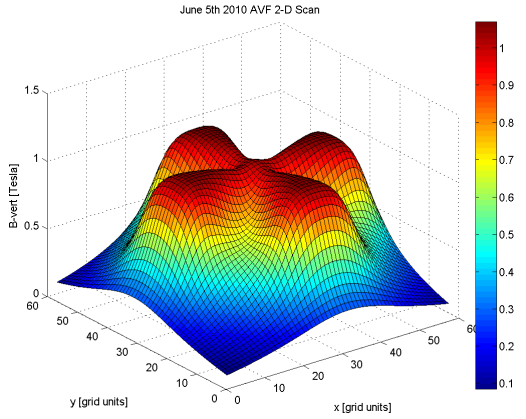

Figure 11. First measurement data from the 2-D scan of the radial sector pole tips. Measurement step are 0.25 inches.

The first set of AVF pole tips measured were of the simplest design, and are shown installed with the cyclotron chamber removed in figure 10. With a periodicity of four, the hills and valley are each 45 degrees wide. They maintain a constant thickness out to the pole edge, except for a ¼ -inch chamfer to break the sharp corners. The data from the first scan is plotted in Figure 11. The four hills are prominent, however a small central bump is observed from the slug that ties the four vanes together. This weak focusing is required to promote a centrally localized focusing field since the flutter will be too small to be effective at the central convergence.

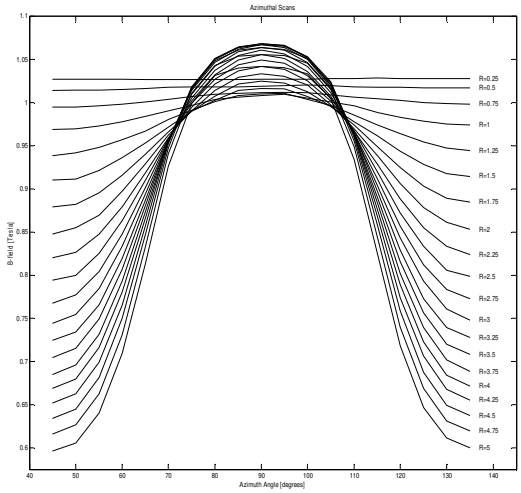

Figure 12 B_z plotted for a sequence of radii in one 90° quadrant displaying the evolution of the flutter with radius.

Figure 12 plots $B_z(\theta)$ over one quadrant displaying the relative evolution of the flutter with radius by individually plotting $B_z(\theta)$ for sixteen radii. The plot shows the emerging sinusoid flutter, despite the square stepped transitions between hills and valleys. Only for radii of 4-inches and greater does a 'flat-top' become apparent.

SIMULATIONS Form start to finish, four software tools have been employed to simulate the beam dynamics of in these magnetic fields. SolidWorks was used to mechanically model the magnet, Maxwell 3D was uses to solve the field problem and generate the needed field report for SIMION to fly and track the ions in. Post processing was performed in MatLab. Details of the Maxwell 3D and SIMION components of the design project follow.

Maxwell 3D (M3D) was first benchmarked against our weak focusing PSF simulations. A 3-D magnet model, which included the weak focusing pole tips was designed in SolidWorks and then imported into Maxwell 3D. The problem was solved to have a nominal peak central field of 1 Tesla. To within measurement errors the models agreed. The next step was to model the simple radial sector pole tips. A B_z-field report was extract from Maxwell 3D over the same range of the above measurement.

A comparison between the AVF 2D measurement and the Maxwell 3D simulation showed good agreement. The measurement was performed with the magnet current set to 45,000 amp-turns, for a peak central B_z of 1 Tesla.

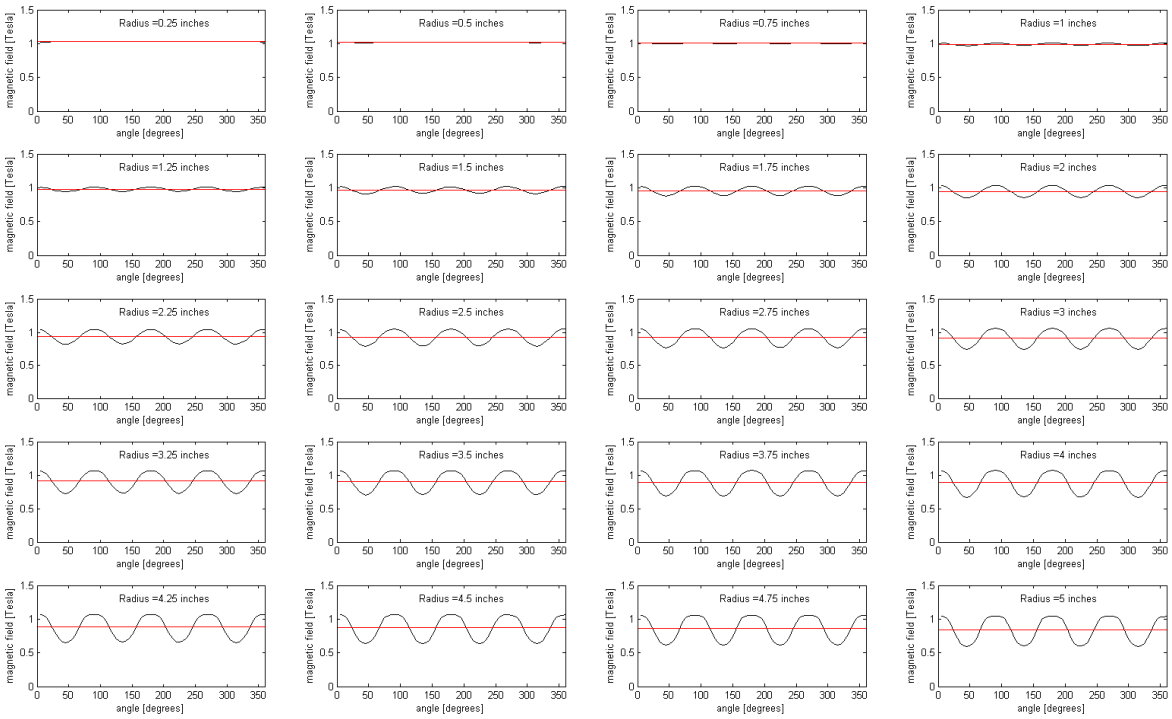

Figure 13. Analysis of Radial AVF pole tips at increasing radii in increments of 0.25 inches. The black traces are B_z as a function of azimuth, and the red traces are the average value about that radius.

The Maxwell 3D current was nearly set the same, differences between the two resulting average field reports were aligned by normalizing the simulated data central B_z value to exactly match the measured central value.

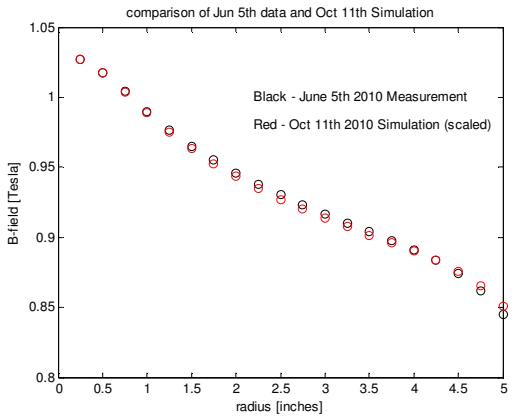

Figure 14. Comparison of measured and simulated average field of the radial sector tips. Good agreement is noted over the range of the ions travel, at most 1% deviation is seen at r=2.5.

The simulated data report was formatted to match the measured data format, so as to use the same MatLab analysis code for both. Figure 13 shows there is at most a 1% deviation between the measured and simulated average field profiles.

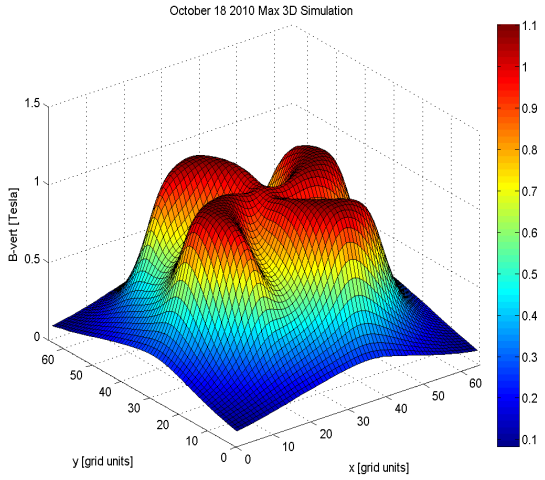

Figure 15 A plot of B_z for the first spiraled poles.

With acceptable agreement between the measurement and simulation, a spiral sector pole was simulated; again each vane had 45° angular width. The spirals were describe by an Archimedes spiral of the form $\theta=\alpha r$, where α=15°. The plotted B_z of the simulated data is shown in Figure 15. And for comparison to Figure 12, B_z is plotted for a sequence of radii in

one 90° quadrant in Figure 16. This shows the procession of the hill and valley with radius.

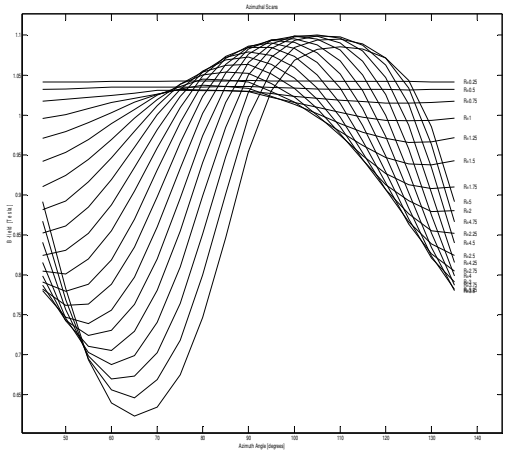

Figure 16 Bz is plotted for a sequence of radii in one 90° quadrant of the simulated spriral pole tips.

SIMION In order to determine the orbit characteristics of a magnetic field, ions with varying initial conditions are launched in the simulated field. The ions' subsequent motion is recorded to establish the limits of the stability in both the radial and axial directions. The code chosen for the task is SIMION, a full 4-D E&M code.[9] SIMION has the capacity to fully model our 12-Inch cyclotron, including the RF aspects and physical apertures. For the following stability investigation the accelerating RF was turned off, but the aperture of the DEE structure was retained. Such simulations are referred to as 'static.'

SIMION imports externally generated electric and magnetic fields, such as Poisson-Superfish 2-D fields, which are then rotated by SIMION (in the case of cylindrical symmetry), or full 3-D fields generated in Maxwell3D (M3D) which require no symmetry. In the following, a full M3D field report is generated. The resolution of the imported field has been set at 1 mm to conveniently match the 1mm:1 SIMION grid unit ratio. The M3D report file is a 6-column a comma separated variable file reporting x, y, z, B_x, B_y, and B_z at each grid point, with a spacing of 1-mm between grid points. To fully cover the ion accessible region in our cyclotron, the field region must span a volume with a radius up to 4.5 inches – the point of interception of deflector. Therefore the extent of the report spans ±115 mm (~ 4.55-inches) x ±115 mm x (~ 4.55-inches) x 53 mm (~ 1.04-inches) which contains 231 x 231 x 53 rows of data, an excess of 2.8 million points - causing the simple text data to become unwieldy, in excess of 500 MB.

A complication arose from the different axis orientations between Maxwell 3D and SIMION. The Maxwell 3D magnetic field's median plane is the x-y plane while the median plane is y-z in SIMION. A careful vector rotation is required in translating the M3D report into the usable SIMION file.

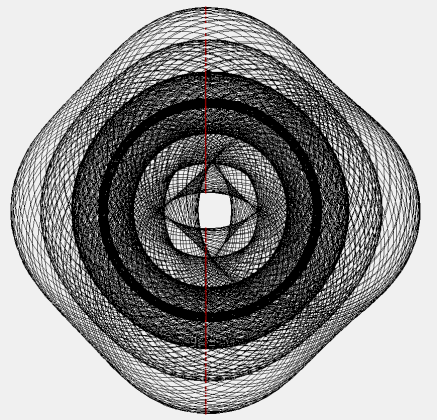

Figure 17 SIMION display of the median plane of four 50 keV ion circulating in the radial sector AVF field. Each red dot indicates an instance of data recording.

Further, SIMION requires that the external field be reported in a .csv format containing a one-line header followed by three columns containing only the three field components. The coordinate of each set of field vectors is encoded in the row number. The first row contains the lowest valued coordinate, i.e. $\{x,y,z\}=\{-26,-115,-115\}$; and the last row of data contains the highest valued coordinate, i.e. $\{x,y,z\}=\{26,115,115\}$. While the magnetic field is being loaded, SIMION populates the vector field by cycling through x the fastest, y the second, and finally z. This requires data sorting that cycles through x for every increment of y, and cycles through y once per increment of z. As a matter of course, z only cycles once. The one-line header contains starting point, size and scaling information, as well as indicators of symmetry, rotation and offset.

After launching the ions, SIMION tracks the particle through the simulated magnetic field. A typical display is shown in Figure 16 where four 50 keV ions were launched in the median plane, each at different radii. While it is possible to record the full $\{x,y,z,t\}$ history of each ion at a resolution as fine as the computational time step, it is impractical to do so. The file size quickly becomes impossible to handle, thus a more manageable characterization is needed.

The figure of merit used to quantify stability of each simulated magnetic field and compare between geometries is *trace space*, a time independent record of the particle behavior.

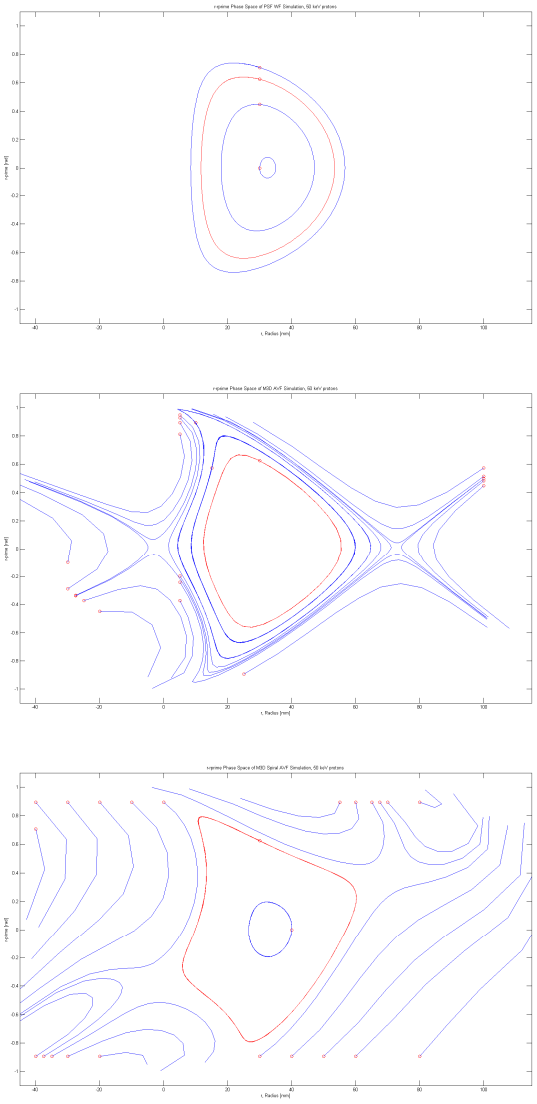

Figure 18. Radial Trace Space plots of 50 keV protons in the weak focusing field (top), radial- (middle), spiral- (bottom) sector AVF fields respectively.

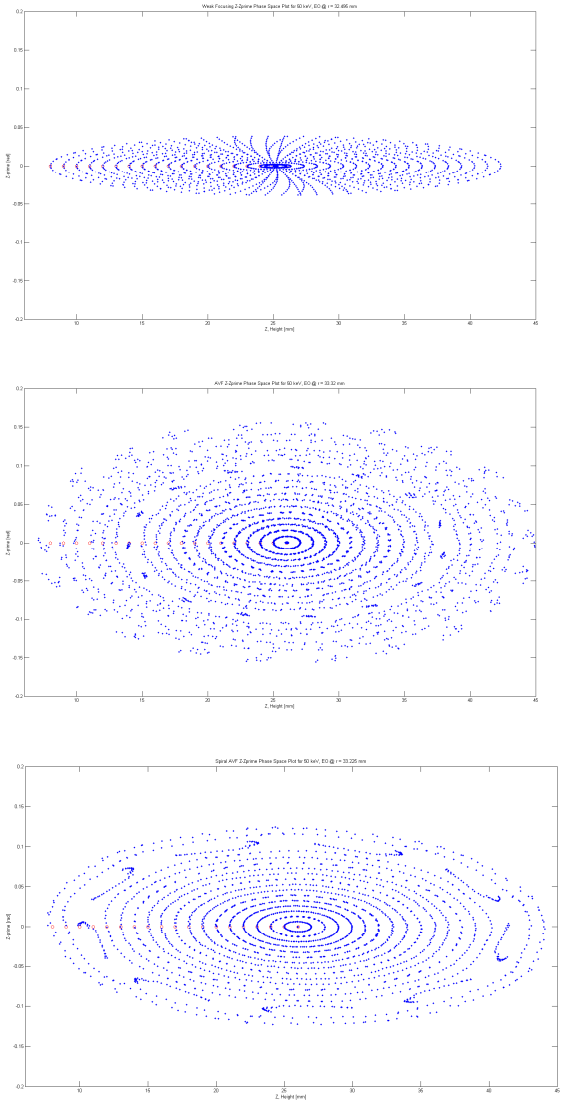

Figure 19. Vertical Trace Space plots of 50 keV protons in the weak focusing field (top), radial- (middle), spiral- (bottom) sector AVF fields.

Trace space correlates a particles position and angle with respect to the ideal orbit tangent (a measurement of transverse momentum) each time it crosses a reference plane.

This is related to the more standard phase space, where position and transverse momentum are correlated. Since the Rutgers 12-Inch Cyclotron is far from the relativistic regime, trace space and phase space are equivalent sans scaling. SIMION provides a suite of predefined data recording options and criteria and was configured to record each particle's 6D vector including $\{x,y,z,v_x,v_y,v_z\}$ as well as the absolute velocity. This data is recorded at the ions start, and every instance of crossing a defined reference plane, such as the $z=0$ plane.

Typically, ions cross the reference plane twice per revolution; post processing sorts the data, focusing on the positive crossing direction, i.e. $-z \rightarrow +z$, while ignoring the $+z \rightarrow -z$ crossing direction. Multiple ions can be launched together, however for these trace space simulations it was found best, especially while searching for the stability limits, to track single ions. The SIMION simulation run terminates once the ion is lost. An ion is declared lost if it exceeds the boundary of the DEE structure or falls outside of the magnetic field volume. If the ion's orbit is stable, it will continue to circulate indefinitely and the simulation will need to be manually terminated. The simulation is interrupted once sufficient data has been collected to populate the trace space curve.

Trace Space Plots Post processing code was written in MatLab for sorting and plotting the recorded data. Initially, three simulations were performed to compare the behavior of 50 keV ions in three magnetic fields. The fields include a simulation of the existing weak focusing magnetic field, the simulation of the existing radial sector field, and a test-case simulated spiral field. This spiral tip was not built.

Radial trace space was explored before the axial (vertical) trace space in order to identify the radial equilibrium orbits. The vertical stability was then explored by launching a vertical distribution of mono-energetic ions at their equilibrium orbit.

Figure 18 shows the trace space of the three magnetic field cases; the scales are identical in each plot. The red circles indicate the starting location of each ion illustrating the "flow." Each plot has one red trace space curve, which represents an ion with identical initial conditions in each plot – comparing relative trace space areas between the three.

Once the radial equilibrium orbits were identified, the vertical stability for the 50 keV ions was examined for each field configuration. A uniformly-spaced vertical sequence of 50 keV ions was launched on the EO, the sequence started at the bottom of the DEE interior - the maximum vertical displacement possible. The ions were flown until most of the trace space contours were completed. As is seen in figure 18, the weak focusing field had the smallest trace space area, the radial AVF had the greatest, and the spiral AVF field was slightly less than the radial sector. It is also interesting to note the appearance of the grouping in several of the incomplete trace space contours, this indicates that the ratio of vertical fraction of an oscillation to the revolution frequency is near a rational fraction, however, given sufficient time they would completely fill in their contour. These trace space orbits are exhibiting near-resonant behavior of the order of the grouping number.

Perhaps a more instructive manner in which to understand the vertical focusing behavior is to track two protons with identical initial conditions but each launched in a different field. This was done using the same weak and pure radial sector field configurations of the above trace space plots. Again 50 keV protons were flown, in both cases they were launched in the median plane and on their EO, however, with a vertical angle.

As is seen in Figure 20, the maximum vertical excursion of the proton in the weak field was nearly four times that of the proton in the radial sector AVF field. This has two immediate implications. First, to accommodate a given ion source, the magnet gap of AVF field can be drastically reduced, implying a smaller and less expensive magnet. Alternatively, the magnet gap can be maintained, and a greater vertical angular distribution can be accepted, implying greater beam intensity at the periphery. Also note the increase of frequency of vertical oscillations per unit time for the case of stronger focusing. This demonstrates the concept of tune, (ν_z in this case) in that the frequency of oscillation is proportional to focusing strength.

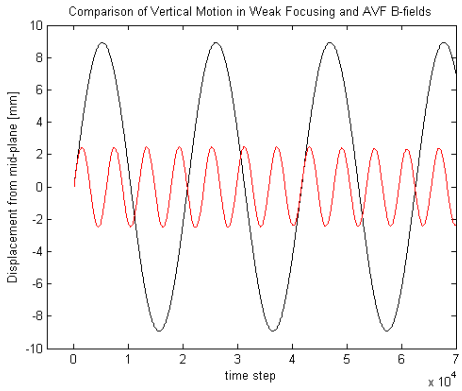

Figure 20, Comparison of two 50 keV protons launch with the same vertical angle on their EO. One in the weak focusing field (black), and the other in the radial sector AVF field (red).

ACCELERATED BEAM SIMULATION

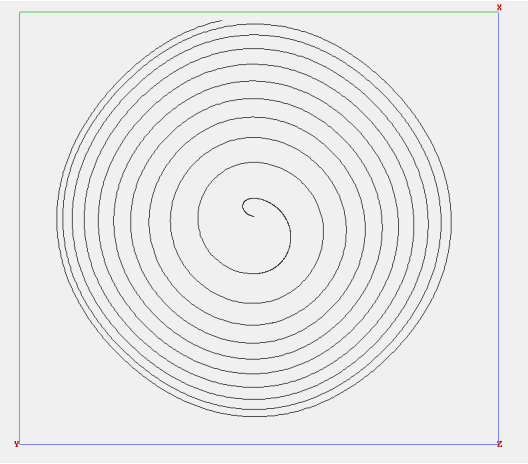

Figure 21. Simulation of a proton accelerated to the periphery in radial sector AVF field. DEE voltage is 20 kV-peak. Note scalloping of the circular orbits

While the constructed radial sector pole tips were not intended to support acceleration, with sufficient DEE voltage protons were successfully accelerated. The incurred phase slippage at normal operating conditions - namely a DEE voltage of 8 kV-peak - was indeed too severe to successfully bring ions to the full radius. However, a DEE voltage of 20 kV peak accepted ions over 20° of the RF cycle and accelerated

them to the periphery. This suggested that our first attempt is not too far from a practical design. Figure 21 shows a single proton accelerated by a DEE voltage of 20 kVpeak.

SPIRAL AVF DESIGN Finally, we present the optimized design for a set of spiral pole tips that are intended to guide beam. The result was a four sector Archimedean spiral sweeping 270 degrees, and will herein be referred to as AKG270. With the exception of the weak focusing central region, these pole tips aimed to satisfy the isochronous condition, in order to minimize the phase slippage, and reduce the minimum DEE voltage while preserving axial stability throughout the accelerating region.

Figure 22. Archemdian Spiral poles that sweep 270° from the center to the periphery.

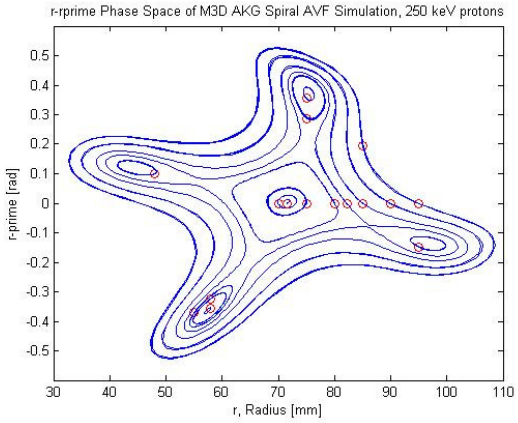

Figure 23. Trace space plot of 250 keV protons indicates five stable orbits. One concentric with the magnet center and four symmetrically located off center.

The AKG270 radial trace space was explored first to identify the equilibrium orbits in 50 keV increments. Even, at 50 keV, non-linear behavior is noted in the larger stable orbits, exhibiting four-sided contours, behavior which is consistent with pole tips that have a sector periodicity of four. The corners of the four-sided nonlinear orbits become more pronounced and bulbous with increasing energy. By 250 keV four closed contours formed in the protracted corners, displayed in Figure 23. Thus, in addition to the primary Equilibrium Orbit, there are four off-center stable orbits. These satellite orbits were confirmed with SIMION, and are shown in Figure 24. Appendix I compiles the radial trace space for a range of energies. Each plot displays six contours. The inner most contour identifies the equilibrium orbit, and the outer most contour is within 5% of the greatest stable orbit.

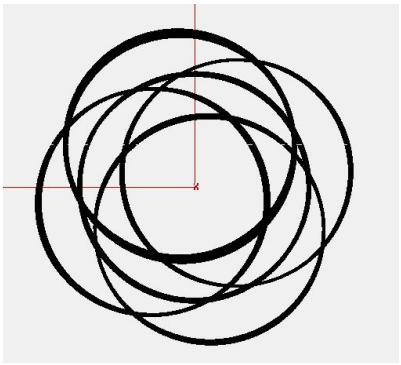

Figure 24. SIMION configuration space display of five 250 keV ions, one launched on each of the stable orbits.

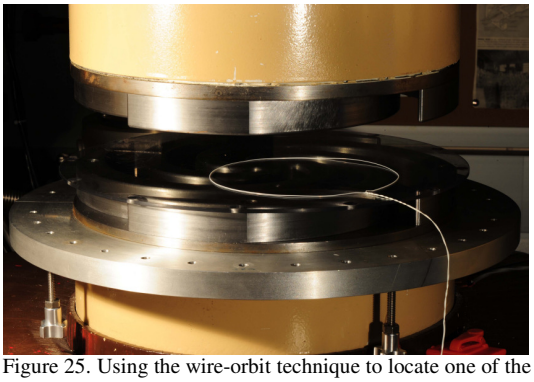

Figure 25. Using the wire-orbit technique to locate one of the five stable orbits.

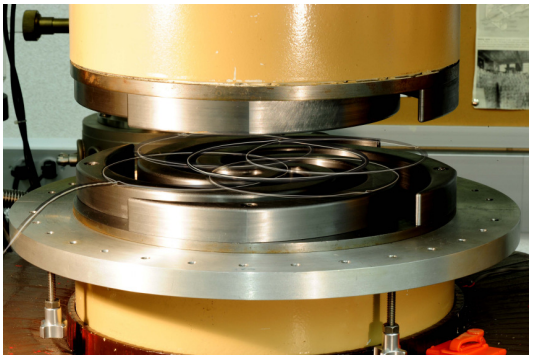

Figure 26. A compostive image of the wire-orbit technique displaying all of the five stable orbits.

The off-center equilibrium orbits were experimentally verified using the wire-loop orbit technique.[7] A 30 AWG wire loop, with a circumference of 71 mm, was energized with a current of 2.5 amps and placed in the magnet gap. Myriad other stable orbits made it difficult to perform this experiment in the median plane; instead a clear acrylic sheet was placed on the bottom pole tip to provide a flat surface on

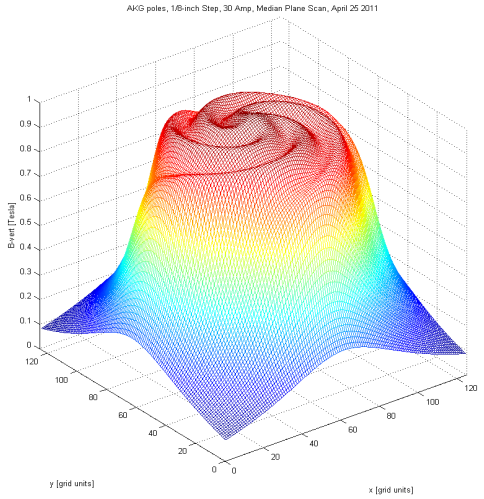

Figure 27. Two dimensional scan of the vertical field component in the median plane.

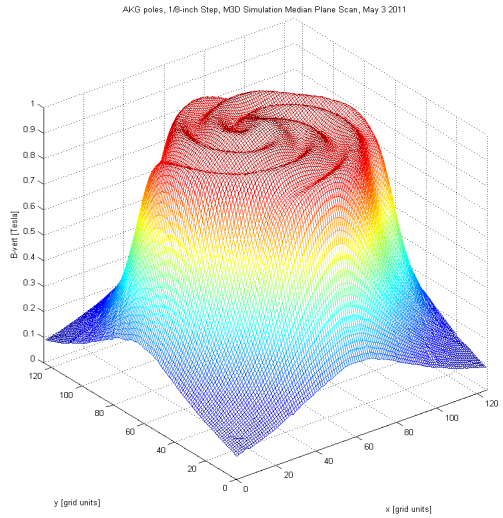

Figure 28. Equivalent "scan" from M3D simulation the vertical field component in the median plane.

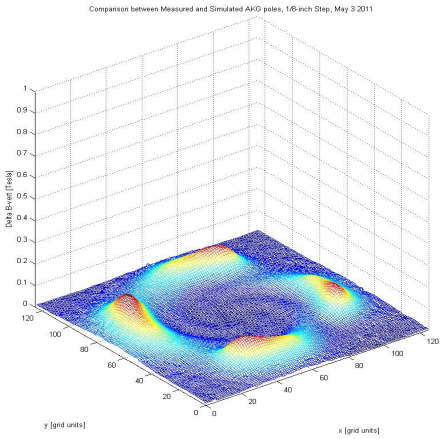

Figure 29. Subtracting the measurement from the simulation reveals 14% discrepancies at the outer pole tip edge. The two agree within 1% in the ion region.

which the wire loop could lay. The energized wire loop simply needed to be tossed towards the gap and it would reproducibly snap to the nearest stable orbit, one such off-center orbit is show in figure 24. An overlay of five loop images demonstrating five stable orbits is shown in figure 25. This technique found another four orbits (for a total of nine) located even further away from the center. Since the wire-loop technique does not discriminate based circumference (only the loop's tension will vary), the further outlaying orbits are most likely lower energy equilibrium orbits.

After locating the equilibrium orbits, a complete comparison of the focusing between the AKG270 poles and the weak focusing pole tips was performed using the simulated fields. The DEEs were removed from both cases to observe, if any, non-linear effects at large excursions. The radial and axial results are respectively shown in Appendix II-a and -b. In most of the radial cases the AKG270 radial trace space is bounded by the weak focusing pole tips. At the lower energies of 50 and 100 keV, the vertical trace space of the AKG270 poletips is larger than that of the weak focusing poles, indicating a greater angular acceptance from the ion source. This is due to the enhanced central focusing from the weak focusing bump.

SPIRAL TIP MEASUREMENTS The final phase of this effort was to measure the vertical field in the median plane and compare with the Maxwell 3D simulation. As seen in figures 27 (measurement) and 28 (simulation) there is good agreement. Both plots were normalized such that the peak central fields were 1 Tesla – this required at most a 5% adjustment to either data set. Figure 29 subtracts the measurement from the simulation.

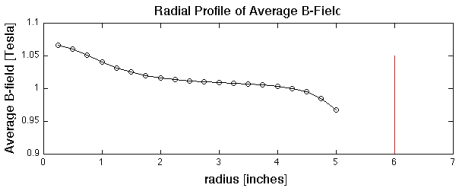

Figure 30. Average Bz as a function of radius for the AKG270 pole tips in the median plane.

Protons were flown with RF in SIMION with the AKG270 magnetic field. The trajectory of a single proton is shown in Figure 21. The driving frequency and amplitude were iteratively tuned to locate the minimum peak DEE voltage necessary to successfully accelerate the proton to the target. This lowest practical voltage found in the simulation was 6 kV_{peak} at a frequency of 15.534 MHz.

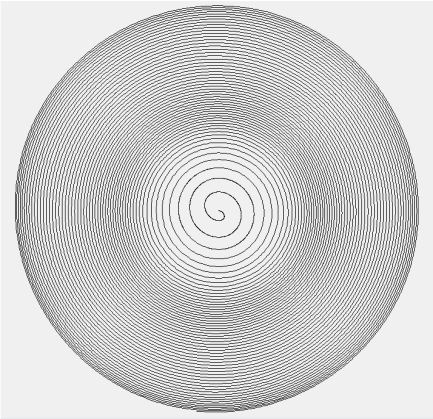

Figure 31. SIMION simulation of successful proton acceleration with a DEE voltage as low as 6 kV_{peak}

FUTURE In parallel to this project, our group has been developing a PIG Ion Source for increased beam intensity. This project is nearing completion and will be tested with both the AKG270 and weak focusing pole tips. The project slated for Spring 2012 will develop a beam phase measurement probe. This experiment measures the beam arrival time with respect to the RF cycle. Measuring variations in the beam's arrival time along a radial line is a method of characterizing the field's isochronism.

At the time of this writing, the authors are exploring an FFT based method to derive the radial and axial tune values from the SIMION simulations. Such a method would be quicker in the evaluation of the magnetic field configurations, reserving the tedium of trace space plot generation for only the most promising candidates.

CONCLUSIONS We have developed a set of pole tips to compare an azimuthally varying field with weak focusing field. The AVF pole tips were designed to use weak focusing in the central region, and use the AVF fields for the needed axial focusing while maintaining isochronism for the remainder of the field. This was accomplished. The radial trace space has revealed stable orbits that reside offset from the central axis, and have been experimentally verified with a wire-orbit.

ACKNOWLEDGEMENTS The authors would like to thank Professor Mohan Kalelkar for arranging the necessary funding to execute this work. We are also indebted to Professor Timothy Antaya for much useful discussion and guidance. We are also thankful to the Physics and Chemistry Machine shop for their perseverance in cutting the complex curves of the pole tips.

REFERENCES

[1] T. Feder, "Building a cyclotron on a shoestring," *Physics Today*, November 2004

[2]http://www.physics.rutgers.edu/cyclotron/papers/12_inch_magnet_studies_4.pdf

[3]http://www.physics.rutgers.edu/cyclotron/papers/Betatron_Studies.pdf

[4]L.H. Thomas, *Phys. Rev.* **54**, 580 (1938)

[5] M. Craddock, "AG Focusing in the Thomas Cyclotron" Proceedings of the 2009 Particle Accelerator Conference, Vancouver, British Columbia, May 4 – 8, 2009

[6] J.J. Livingood, "Principles of Cyclic Particle Accelerators," D. Van Nostrand, 1961

[7]http://www.physics.rutgers.edu/cyclotron/papers/ion_source_studies_part_1.pdf

[8]http://www.physics.rutgers.edu/cyclotron/papers/IonSourceStudiesII_march_26_2008.pdf

[9]SIMION

[10] H.L. Anderson and J. Marshall, University of Chicago, Synchrocyclotron Progress Report, I (July, 1947-July, 1948); II (July, 1948-July, 1949); III (July, 1949-July, 1950)

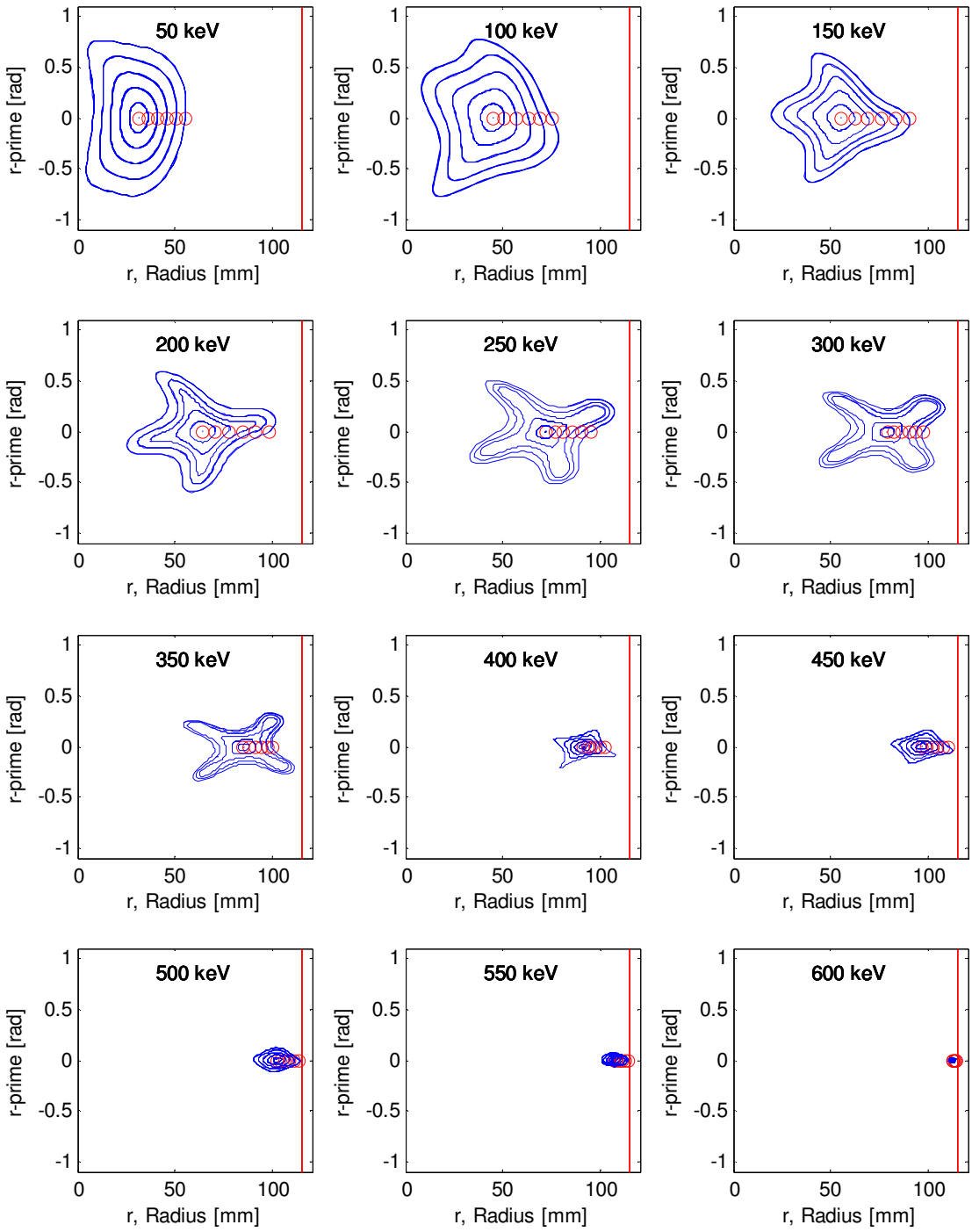

Appendix I. Static radial trace space plots computed for protons in the AKG270 pole tip configuration using the Maxwell 3D model. The red vertical line denotes the hard edge drop off of the field used to fly the ions and may artificially impose a smaller radial aperture for ions of energy 500 keV and greater.

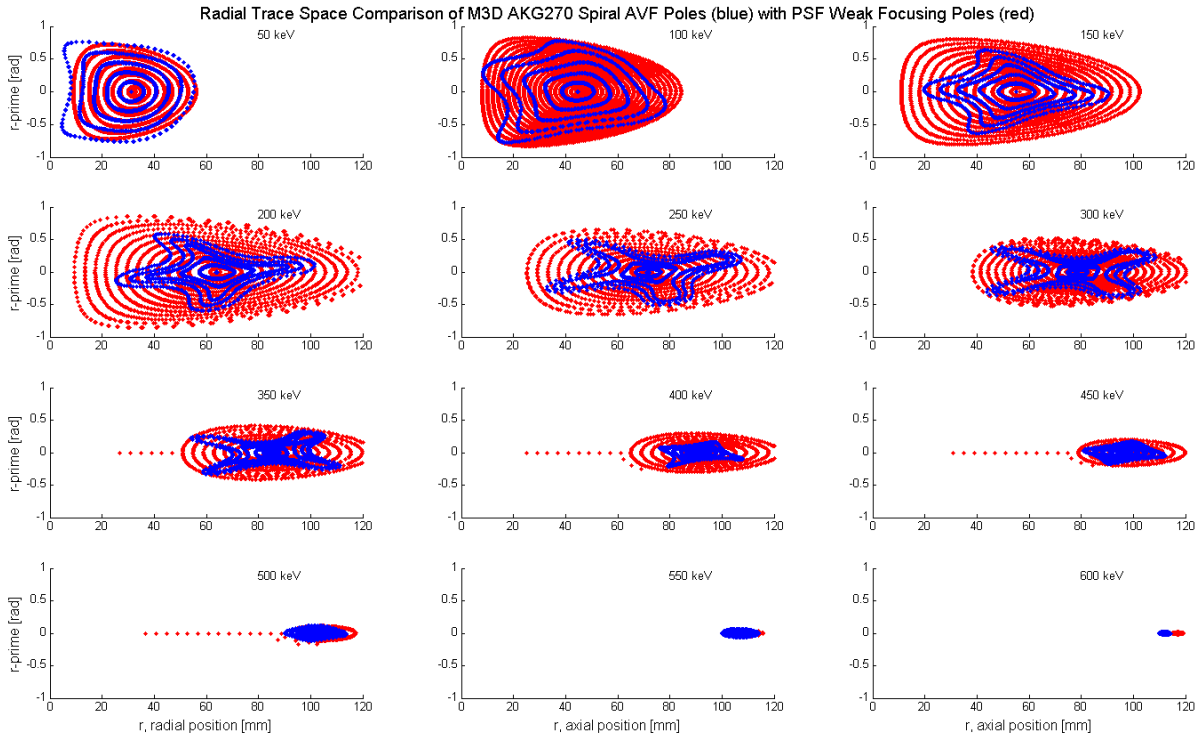

Appendix IIa. Static radial trace space plots computed for protons in both the standard weak focusing field (red) and the AKG270 AVF spiral field (blue).

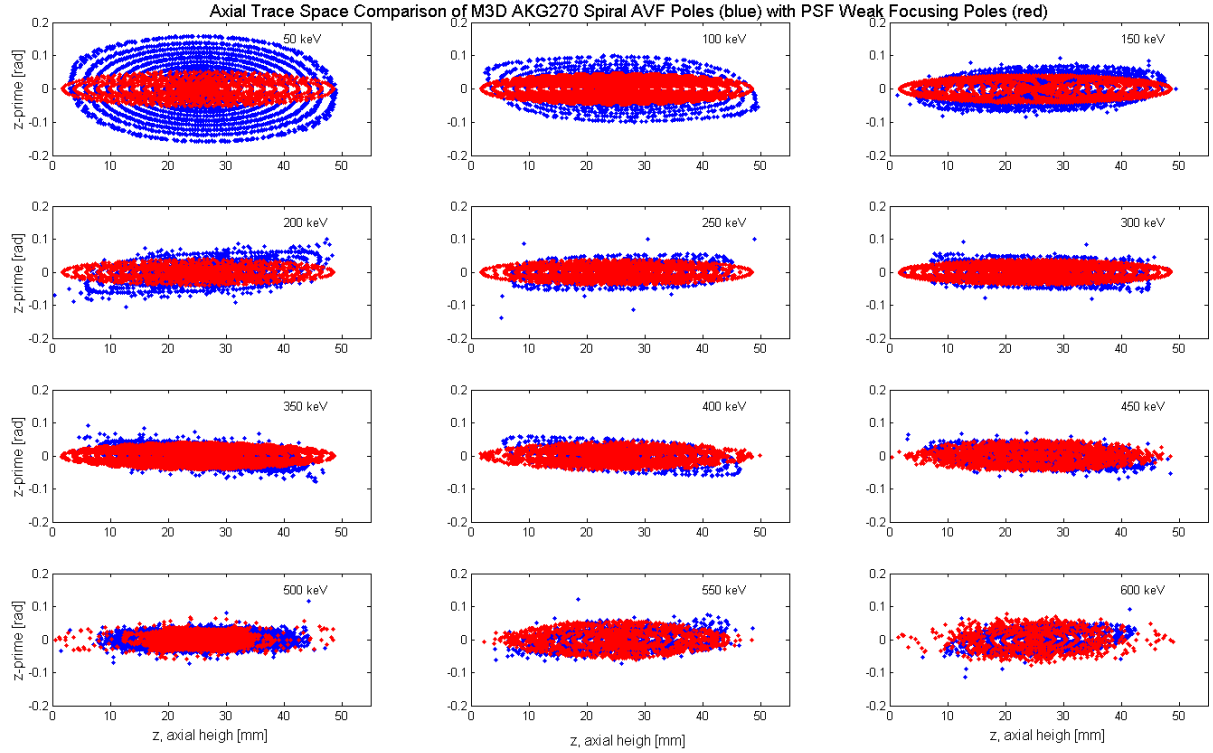

Appendix IIb. Static axial trace space plots computed for protons in both the standard weak focusing field (red) and the AKG270 AVF spiral field (blue).